



Pulsed chemical vapor deposition for crystalline aluminum nitride thin films and buffer layers on silicon and silicon carbide

Aaron J. McLeod^a, Scott T. Ueda^b, Ping C. Lee^b, Jeff Spiegelman^d, Ravindra Kanjolia^c, Mansour Moïnour^c, Jacob Woodruff^c, Andrew C. Kummel^{a,*}

^a Department of Chemistry and Biochemistry, University of California San Diego, La Jolla, CA 92093, USA

^b Materials Science and Engineering Program, University of California San Diego, La Jolla, CA 92093, USA

^c EMD Electronics, San Jose, CA 95134, USA

^d Rasirc, Inc., San Diego, CA 92126, USA

ARTICLE INFO

Keywords:

Aluminum nitride
Chemical vapor deposition
X-ray diffraction
X-ray photoelectron spectroscopy
Transmission electron microscopy

ABSTRACT

Low temperature aluminum nitride (AlN) deposition has applications ranging from serving as a heat spreading material to serving as a buffer layer for III-V semiconductors on silicon or silicon carbide (SiC) for radio frequency, power, and microLED devices. While crystalline AlN is traditionally deposited at high temperature (>800 °C), in the present study AlN is deposited on Si(100), Si(111), and 4H-SiC substrates by two modest temperature processes using a metal precursor with high thermal stability, tris(dimethylamido) aluminum (III), and a highly reactive nitrogen source, anhydrous hydrazine. A 580 °C pulsed chemical vapor deposition (CVD) process is compared to a more complex 400 °C atomic layer annealing process, in which the same precursors are utilized with periodic ion bombardment to induce film crystallinity. Films deposited by both processes template preferential c-axis orientation in subsequently sputtered AlN on unheated substrates. Both templating techniques demonstrate equivalent enhancements in crystallinity of the sputtered AlN relative to a non-templated sputtered film by x-ray diffraction and transmission electron microscopy studies. On 4H-SiC substrates, a comparison of sputtering directly and templating with the 580 °C pulsed CVD process reveals epitaxial deposition by the 580 °C pulsed CVD process which extends into the low temperature sputtered AlN.

1. Introduction

Aluminum nitride (AlN) is a promising material due to its high thermal conductivity and close lattice match to gallium nitride (GaN) and indium gallium nitride (InGaN). Accordingly, AlN may find application as a heat spreading material and/or as a buffer layer material [1–7]. Deposition methods for crystalline aluminum nitride typically require temperatures exceeding 800 °C, such as metal organic chemical vapor deposition (MOCVD) and molecular beam epitaxy (MBE); this presents barriers to integration in back-end-of-line processing [8–10]. For application of AlN as a buffer layer for the growth of GaN and InGaN on silicon (Si) and silicon carbide (SiC), high-quality crystalline AlN films with c-axis orientation are necessary [7,11,12]. Deposition methods at comparatively lower temperatures (~350 °C), such as plasma-enhanced ALD (PE-ALD) and atomic layer annealing (ALA), can be used to deposit crystalline or polycrystalline AlN with less strain than films deposited at higher temperatures; however, PE-ALD produces

non-stoichiometric AlN films that are often nano-crystalline [13–15]. Atomic layer annealing has recently drawn attention for low temperature deposition of crystalline or polycrystalline AlN, however its practical utility is limited by low deposition rates due to lengthy ion bombardment treatments and the relative complexity of required deposition tools [16,17].

Trimethyl aluminum (TMA) is a common precursor for many deposition methods despite its thermal decomposition at temperatures above 350 °C; this often results in films with substantial carbon contamination and nitrogen poor stoichiometry [18–20]. Tris(dimethylamido) aluminum (III) (TDMAA) and related tris(diethylamido) aluminum (III) (TDEAA) have shown recent promise for higher-temperature deposition, enabling deposition of AlN with minimal contamination to be deposited by ALD and ALA at temperatures above 350 °C [18,21,22]. This work demonstrates the use of tris(dimethylamido) aluminum (TDMAA) at 400 and 580 °C to deposit AlN by a pulsed chemical vapor deposition (CVD) method on non-lattice matched (Si) substrates and lattice-matched (SiC)

* Corresponding author.

E-mail address: akummel@ucsd.edu (A.C. Kummel).

<https://doi.org/10.1016/j.tsf.2023.139717>

Received 31 May 2022; Received in revised form 7 January 2023; Accepted 25 January 2023

Available online 1 February 2023

0040-6090/© 2023 Published by Elsevier B.V.

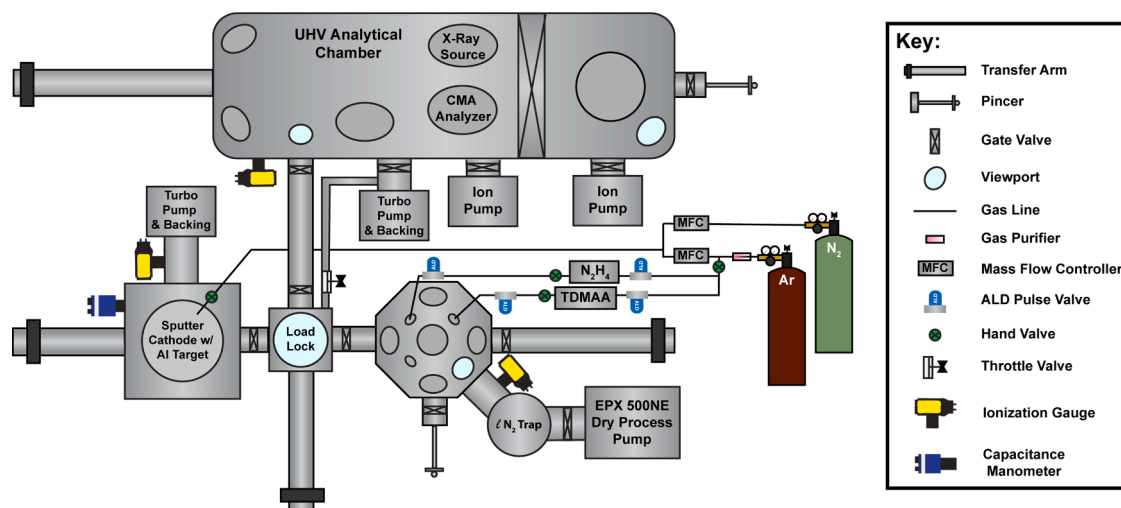


Fig. 1. Chamber Schematic Diagram Chamber schematic showing separate pulsed CVD and ALA chamber (bottom right), sputtering chamber (bottom left), and analytical chamber (top) linked through an in-vacuum transfer system.

substrates in a homebuilt deposition chamber with growth rates up to ~45 nm/h. At 400 °C substrate temperature, the films are nanocrystalline with random crystallite orientation, while at 580 °C the films show growth of columnar grains. Films produced by the pulsed CVD method at 580 °C are demonstrated to template preferential c-axis orientation in additional AlN deposited by reactive sputtering and are compared to sputtered AlN on a template layer deposited by ALA at 400 °C. Both films show a similar result in enhancing AlN (002) orientation. On 4H-SiC, epitaxy is observed by the 580 °C pulsed CVD method, which greatly enhances the crystallinity of low temperature (< 100 °C) sputtered material when used as a templating layer.

2. Materials and methods

2.1. Substrates and preparations

Silicon wafers with (100) and (111) orientations were obtained from WaferWorld. Silicon carbide wafers of 4H polymorph with a 4 off-c-axis cut were obtained from El Cat, Inc. Substrate coupons were degreased using acetone, methanol, and water (Fisher Scientific) and stripped of native oxide by a three-step cyclic etch in 2% HF in deionized water (VWR). Tris(dimethylamido) aluminum (III) was supplied by EMD Performance Materials; anhydrous hydrazine was supplied by RASIRC.

2.2. Chemical vapor deposition system

The pulsed CVD was performed in a homebuilt vacuum chamber (walls heated to 90 °C, base pressure $<1 \times 10^{-4}$ Pa) pumped by an Edwards EPX 500 NE high vacuum pump with an in-line liquid nitrogen trap. A tool schematic is shown in Fig. 1. The deposition chamber is attached to two additional vacuum chambers through an in-vacuum transfer system: the first containing a sputtering system and the second containing an x-ray photoelectron spectroscopy system.

The pulsed CVD process was performed at substrate temperatures of 400 and 580 °C. The TDMAA precursor container was heated to 105 °C for deposition and held at 85 °C for storage. All precursor dosing was controlled by a LabView system and was performed in a manner consistent with ALD: the precursors were pulsed in an alternating fashion separated by brief periods of pumping. The process is denoted as pulsed CVD because the TDMAA precursor did not display self-limiting growth, as is characteristic of ALD processes, for the short pulse times utilized in this study. Similar behavior has been observed for the deposition of AlN using TDMAA and NH₃ [23]. Both precursor containers were pressurized with Ar prior to dosing; trace water and oxygen

Table 1

Pulsed CVD dosing conditions at 400 and 580 °C.

	400 °C	580 °C
TDMAA Dose	150 ms	90 ms
Post-TDMAA Pump	4 s	4 s
N ₂ H ₄ Dose	100 ms	80 ms
Post-N ₂ H ₄ Pump	8 s	8 s

were removed from the Ar push gas using an Entegris GateKeeper purifier. The pulse times used for 400 and 580 °C deposition are shown in Table 1 and were previously optimized to achieve 1.2–1.5 Ang./cyc. growth rates [22].

2.3. Deposited thin films and CVD-templated sputtered films

Table 2 describe the samples deposited for the three studies performed in this paper. An initial set of thin films with 40 nm target thickness were deposited by pulsed CVD on Si(111) and Si(100) at 400 °C and 580 °C to evaluate the effects of lattice mismatch and substrate temperature. A second set of depositions was performed on Si(111) to analyze the templating ability of the 580 °C pulsed CVD relative to a previously reported ALA technique using Ar ions bombardment at -25 V DC substrate bias: a 20–30 nm template layer by either method was first deposited followed by 150–170 nm of sputtered AlN [22]. These two templated films are compared to a reference 190 nm AlN sputtered film deposited directly onto Si(111). A third set of depositions compares the effectiveness the 580 °C pulsed CVD template layers on 4H-SiC to a reference sputtered film; 20 nm and 40 nm template layers were deposited and all samples were brought to a total thickness of 190 nm by reactive sputtering. For all templated samples layer thicknesses are approximate and were based on observed growth rates. Reactive sputtering was performed using a 69% N₂/31% Ar gas mixture (Praxair and AirGas, >99.999%) in a balanced magnetron configuration (Kurt J. Lesker Torus MagKeeper, >99.99% purity Al target) with 100 W DC power operating at 0.43 Pa as measured by a capacitance manometer (Kurt J. Lesker Co.). Samples were not actively heated during sputter deposition, however a thermocouple mounted on the sputtering stage showed increases from 20 °C to 70–80 °C following deposition.

The surface composition of the films was determined by x-ray photoelectron spectroscopy (STAIB Instruments DESA 150 CMA, Mg K α source) of the Al 2p, N 1s, C 1s, O 1s and Si 2p regions. Peak fitting (CASA XPS) was performed using a Shirley background profile and elemental composition was corrected using Scofield relative sensitivity

Table 2
List of sample depositions and deposition methods.

Comparison Set	Sample Description	Substrate	Thin Film or Template Layer Thickness (nm)	Sputtered Layer Thickness (nm)	Placement in Article
Thin Films	400 °C Pulsed CVD	Si (111)	44.6	N/A	See Figs. 2–6
		Si (100)	41.3		
	580 °C Pulsed CVD	Si (111)	43.8		
		Si (100)	44.6		
Templated Films on Si(111)	580 °C Pulsed CVD	Si (111)	31	~150	See Fig. 7.
	400 °C ALA, Ar –25 V DC		21	~175	
	Sputtered Reference		N/A	~190	
Templated Films on 4H-SiC	580 °C Pulsed CVD	4H-SiC	~20	~170	See Fig. 8 and 9
			~40	~150	
	Sputtered Reference		N/A	~190	

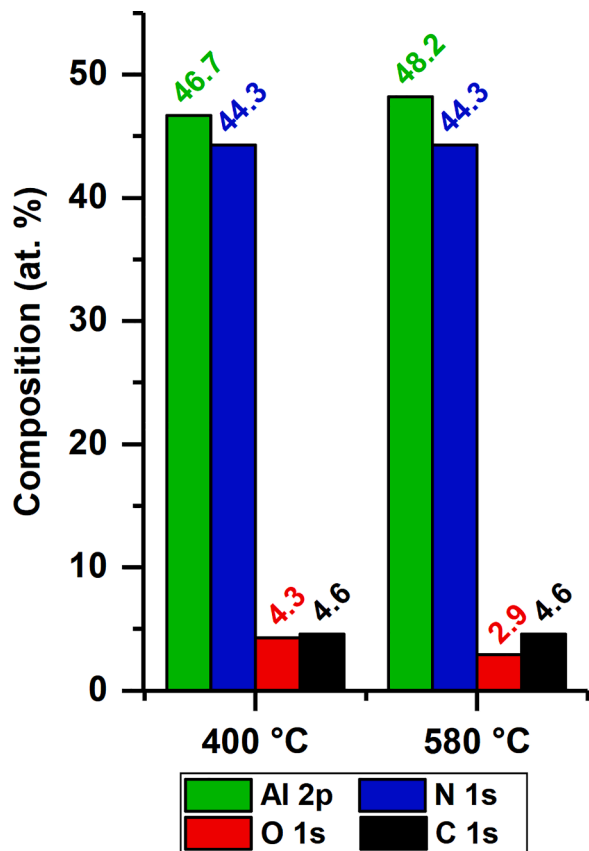


Fig. 2. Composition of Pulsed CVD AlN vs Temperature Film composition data for pulsed CVD at substrate temperatures of 400 °C (44.9 nm thick) and 580 °C (43.8 nm thick) on Si(111) as determined by XPS. Note, these are surface compositions and bulk contaminants may be lower.

factors. All photoelectron spectra were referenced to adventitious carbon at 284.8 eV.

2.4. Characterization

For all film depositions on Si(111) and Si(100), grazing incidence x-ray diffraction (GI-XRD) was performed to analyze film crystallinity and preferred orientation (Rigaku SmartLab, Cu anode operating at 2 kW, parallel beam configuration, fixed 1.005° incidence angle). X-ray reflectivity measurements of the thin film samples from 0 to 3° 2θ were performed on the same instrument and were modeled using Rigaku GlobalFit software to determine film thickness and density. Bragg-Brentano x-ray diffraction was used for films deposited on SiC due to its comparatively lower instrumental broadening; this allowed for resolution of AlN and SiC diffraction peaks that are not easily resolved in

GI-XRD.

Four types of transmission electron microscopy (TEM) were performed: bright field (BF-TEM), dark field (DF-TEM), scanning (STEM), and high-resolution (HR-TEM). Selected area electron diffraction (SAED) was also performed for films on SiC. All lamellae were prepared using a focused ion beam (FIB) milling system with thinning to approximately 40 nm by Covalent Metrology (Sunnyvale, CA). All TEM, STEM, and SAED was performed using a ThermoFisher Talos F200X G2 transmission electron microscope.

3. Results and discussion

3.1. Thin films

Representative composition data as determined by XPS is shown in Fig. 2 for pulsed CVD thin film depositions at 400 and 580 °C on Si(111). At both substrate deposition temperatures, nearly 1:1 stoichiometric Al:N is observed with minimal oxygen and carbon content. The composition information reflects the composition of the top 3–5 nm of the AlN films. In-vacuum transfer of the substrates through the load lock after deposition may result in slight oxidation of the AlN surface, meaning bulk oxygen content is likely lower than is the surface composition determined by XPS and shown in Fig. 2.

Photoelectron spectra and corresponding peak fits used for the determination of film composition of these samples are shown in Fig. 3. The Al 2p regions in Fig. 3a and e are fitted with a spin orbit split binding energy difference of 0.4 eV. The C 1s x-ray photoelectron spectra in Fig. 3d and h indicate adventitious hydrocarbon contamination of the film surfaces due to the presence of peaks at 284.8 eV, 287.3 eV, and 288.5 eV, corresponding to C–C, C–O, and C=O bonds. At both deposition temperatures, no low binding energy peak is observed in the C 1s region indicating the absence of Al–C bonds. These observations suggest that the carbon content in the bulk of these films is likely lower than is observed on the film surface. This low carbon contamination is consistent with previous reports of TDMAA used for deposition of AlN and AlO_x and is attributed to the lack of Al–C bonds in the precursor structure [21].

Note the N 1s spectra are fit using two peaks, as is customary in XPS characterization of aluminum nitride films; the main nitride peak is located at 397.0 eV and the higher binding energy peak at 398.8 eV corresponds to O–Al–N bonds likely present on the oxidized film surface [24]. It is commonly reported that the charge-balanced sum of nitrogen and oxygen content should equal that of aluminum [24]. While the stoichiometry of the bulk AlN was not measured (e.g., by depth profiling XPS), it is likely that the concentration of oxygen and nitrogen in the bulk of the films may equal that of aluminum and the films are, therefore, stoichiometric.

Results from the grazing-incidence x-ray diffraction study are shown in Fig. 4; Table 3 lists the corresponding film thickness and density values, as determined by XRR, and AlN (002) peak full-width at half maximum (FWHM) as determined by GI-XRD. Polycrystallinity with

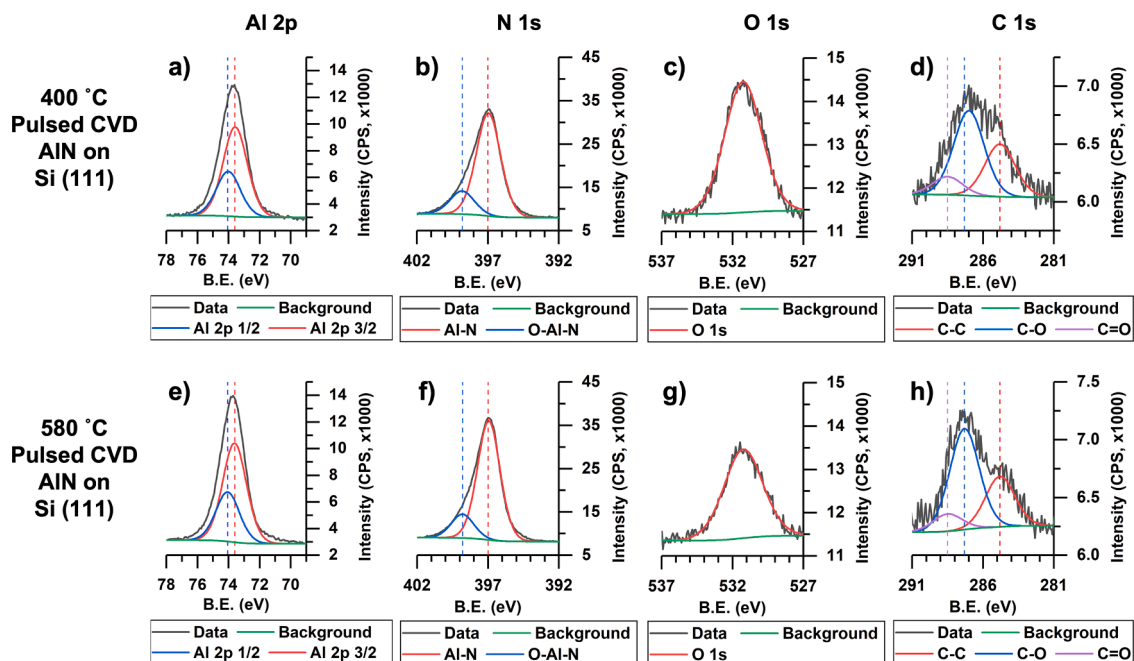


Fig. 3. High Resolution X-Ray Photoelectron Spectra X-Ray photoelectron spectra of the Al 2p, N 1s, O 1s, and C 1s regions for films deposited by (a–d) the 400 °C and (e–h) 580 °C pulsed CVD AlN processes on Si(111).

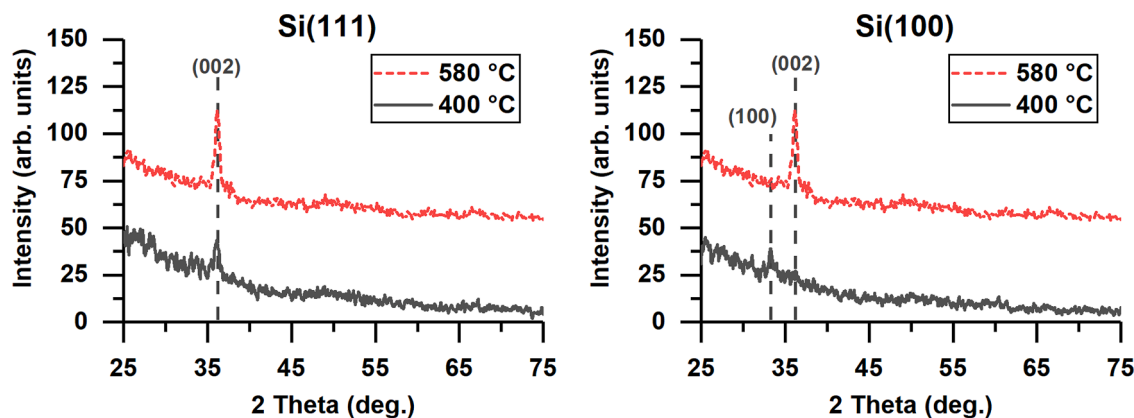


Fig. 4. Crystallinity Analysis for Pulsed CVD AlN vs Temperature GI-XRD patterns for AlN films deposited at 400 and 580 °C by pulsed CVD on Si (111), left, and Si (100), right.

Table 3
Thin film properties as determined by XRR and GI-XRD for Pulsed CVD AlN.

Substrate	Deposition Temperature (°C)	Thickness (nm)	Density (g/cm ³)	AlN (002) FWHM (deg.)	AlN (002) Peak Position (deg.)
Si (111)	400	44.6	2.86	N/A	N/A
	580	43.8	3.11	0.73	36.2
Si (100)	400	41.3	2.59	N/A	N/A
	580	44.6	3.09	0.75	36.1

preferential c-axis orientation is observed on both substrates at 580 °C whereas deposition at 400 °C is nanocrystalline on Si(111) and amorphous on Si(100). On Si (111) (Fig. 4a), crystallinity is observed at 580 °C with a preferred AlN (002) orientation, whereas at 400 °C minimal diffraction signal is observed at the AlN (100) peak position. The full-width at half maximum intensity (FWHM) of the AlN (002) peak on the 580 °C film is 0.73° at a position of 36.2° relative to a theoretical position of 36.1°. This may indicate that strain is present in the film, likely due to deposition on a non-lattice matched substrate. On Si (100) (Fig. 4b), similar crystallinity is observed at 580 °C with an AlN (002)

peak of 0.75° FWHM at an angle of 36.1°. When depositing at 400 °C substrate temperature on Si (100), no crystallinity is detected. The XRR measurement and fit profiles for each film are shown in Fig. 5. The decrease in signal observed beyond 1.5 2θ for the films deposited at 580 °C substrate temperature may be due to increased surface roughness, consistent with the growth of larger crystallites.

As listed in Table 3, the films deposited at 580 °C have greater density than their 400 °C counterparts, with increases of 8.4% and 17.6% observed for the films on Si (111) and Si (100), respectively. It is noted that the largest film density observed, 3.11 g/cm³ for the film

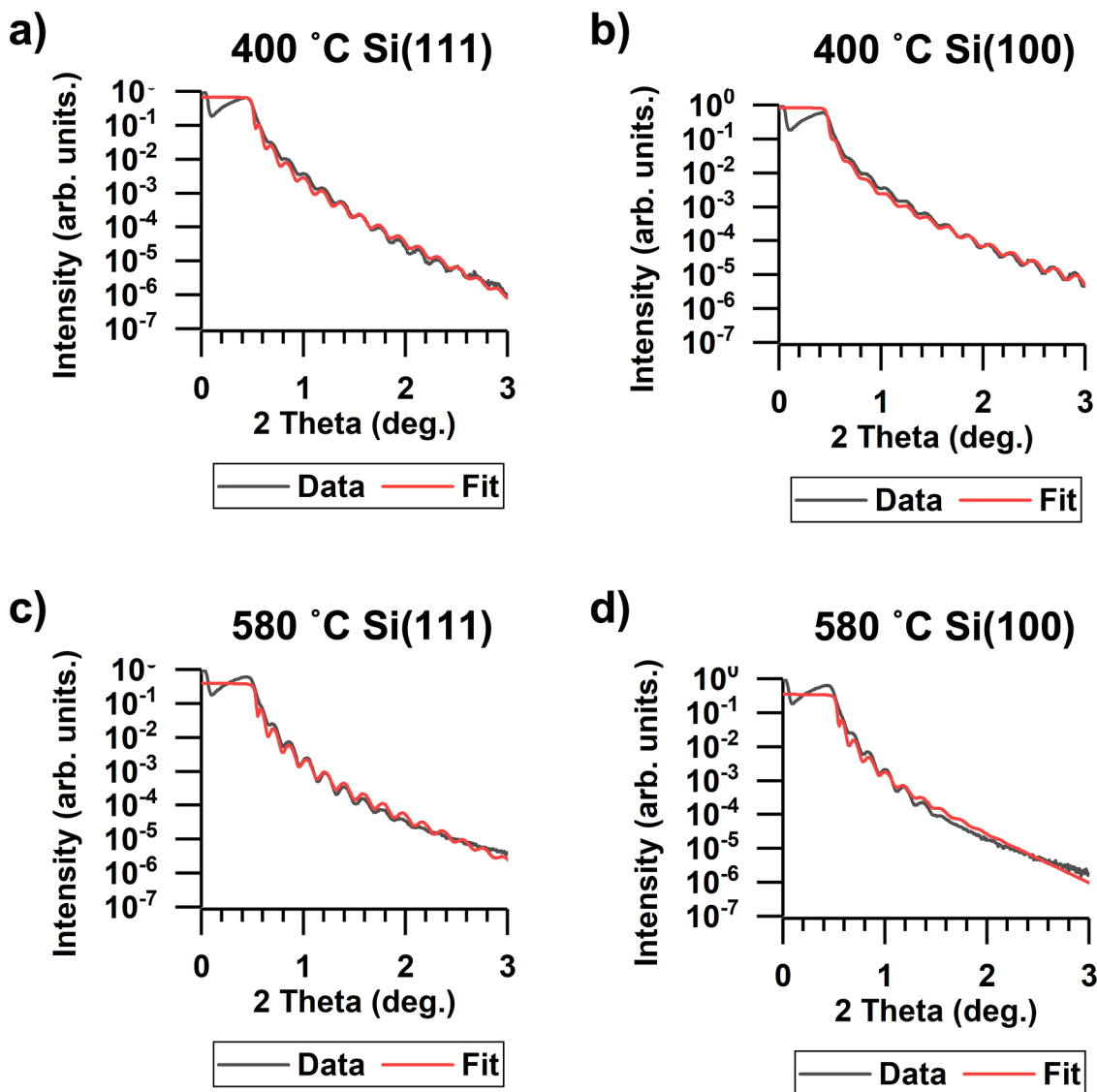


Fig. 5. X-Ray Reflectivity Measurement and Fit Profiles X-Ray reflectivity profiles for the films deposited at 400 °C on Si (111) and Si (100), and at 580 °C on Si (111) and Si(100), panels a, b, c, and d, respectively.

deposited at 580 °C on Si (111), is still less than that of bulk AlN at 3.26 g/cm^3 . This is likely due to the presence of amorphous material at grain boundaries and at the Si-AlN interface.

The data in Figs. 4, 5, and Table 3 demonstrates that moderate increases in substrate temperature during pulsed CVD, such as increasing from 400 to 580 °C, can aid in developing crystalline structure on non-lattice matched substrates. The average crystallite size for any one condition is not limited by thickness as all films with observed crystallinity are of comparable thickness. The differences in crystallinity on Si (111) and Si (100) are consistent with the hexagonal wurtzite structure of aluminum nitride having a closer lattice match to the Si(111) face rather than the Si(100) face [25].

These GI-XRD results are complimented by the electron microscopy and diffraction studies of the thin films deposited at 400 and 580 °C, shown in Fig. 6. Bright field TEM for these films is shown in panels 6a and 6b, respectively. In the micrograph of the film deposited by pulsed CVD at 400 °C, a nanocrystalline film with randomly oriented grains of $\sim 5 \text{ nm}$ diameter is observed. In contrast, the film deposited at 580 °C shows crystallites coalescing and taking on a columnar structure in which the crystallite diameter increases as a function of film thickness. These observations are confirmed by aperture-based dark field TEM

used to highlight separate crystallites, shown in Fig. 6b and c. The 400 °C film appears nanocrystalline with rare instances of columnar grains. At 580 °C, the columnar grain structure noted in bright field TEM is observed across the entire film as is evidenced by the diffraction of several columnar crystallites. When considering the GI-XRD, XRR, BF-TEM, and DF-TEM results altogether, it is evident that the 580 °C pulsed CVD process deposits films with superior crystallinity and more ordered grain structure than those deposited by the 400 °C process.

3.2. Templated sputtered films on Si(111)

For AlN to be utilized as a buffer layer for the growth of GaN and InGaN on silicon and silicon carbide, goals of the RF and microLED industries, thicker layers with c-axis orientation are necessary. In Fig. 7, two samples of 181–196 nm total thickness are compared by STEM and GI-XRD: the first is a 31 nm layer of AlN deposited using the 580 °C pulsed CVD process to template 150 nm of sputtered AlN (red in GI-XRD); the second is a templated film comprised of an initial 21 nm layer of AlN deposited using ALA at 400 °C substrate temperature with 175 nm of sputtered AlN deposited on top (blue in GI-XRD); note the substrate temperature is below 100 °C during the sputtering process.

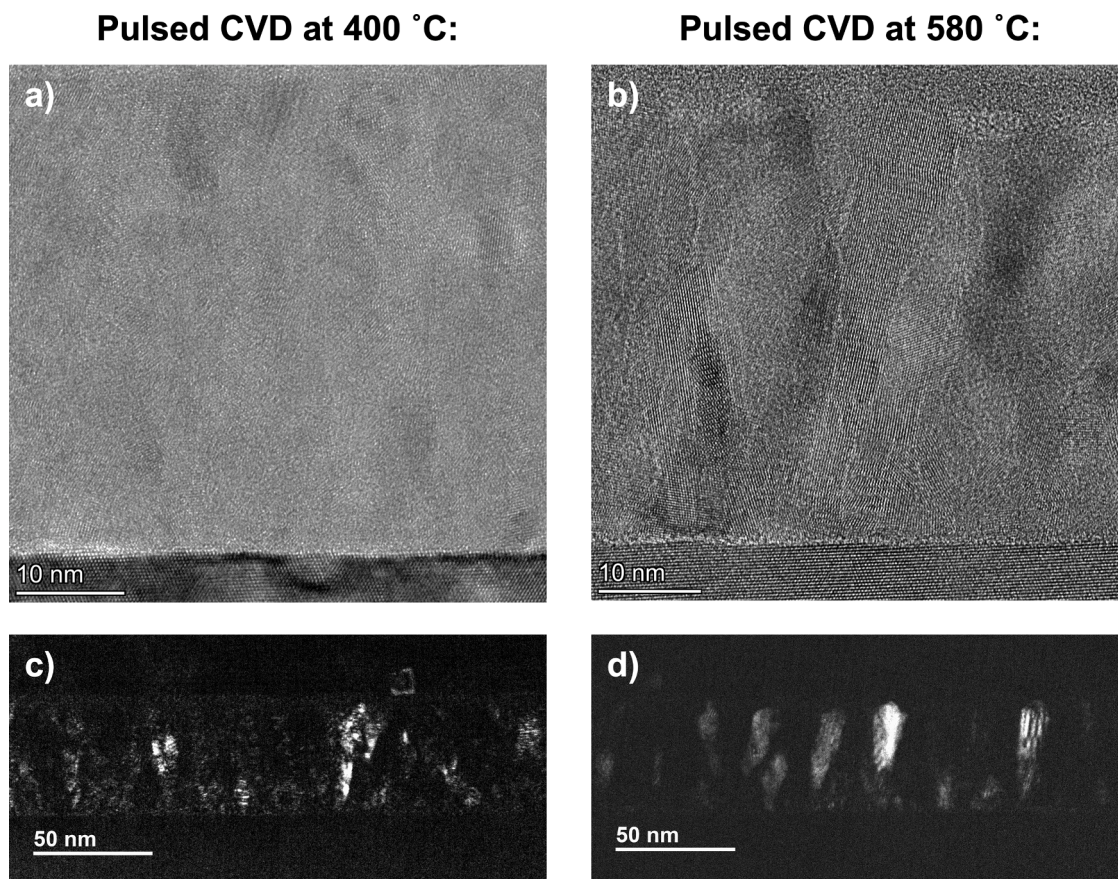


Fig. 6. BF-TEM and DF-TEM of pulsed CVD films on Si (111) BF-TEM (top) and DF-TEM (bottom) of pulsed CVD films deposited on Si (111) at (a,c) 400 °C and (b,d) at 580 °C.

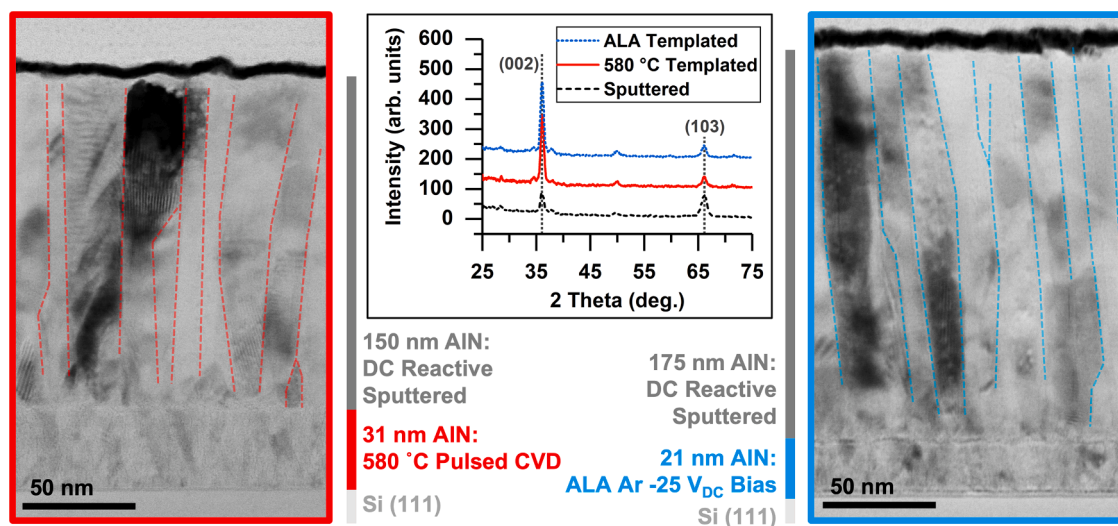


Fig. 7. STEM Comparison of 580 °C CVD and 400 °C ALA Templated Films and GI-XRD Comparisons STEM Comparison of grain structure by STEM in 580 °C pulsed CVD-templated sputtered AlN (left) and 400 °C ALA-templated sputtered AlN (right) on Si(111). Grain boundaries are manually traced in the top sputtered layer to visually aid in comparison.

ALA was performed using a 20 s ion bombardment at the end of each precursor dosing cycle, with Ar ions generated by an inductively coupled plasma source. For this ion bombardment process, the substrate was biased to -25 V DC to accelerate the ions toward the growth surface to crystallize the material. Experimental details can be found in previous works [22,26]. These two templated films are also compared to a

reference film of 190 nm sputtered AlN on Si(111) by GI-XRD (black line in GI-XRD comparison). AlN deposited by this sputtering condition showed 49.4 at.% Al, 42.5 at.% N, 5.1 at.% O, and 3.1 at.% C composition by XPS.

The GI-XRD comparison inset (Fig. 7) shows that AlN (002) orientation is strongly preferred when the sputtering is performed on either

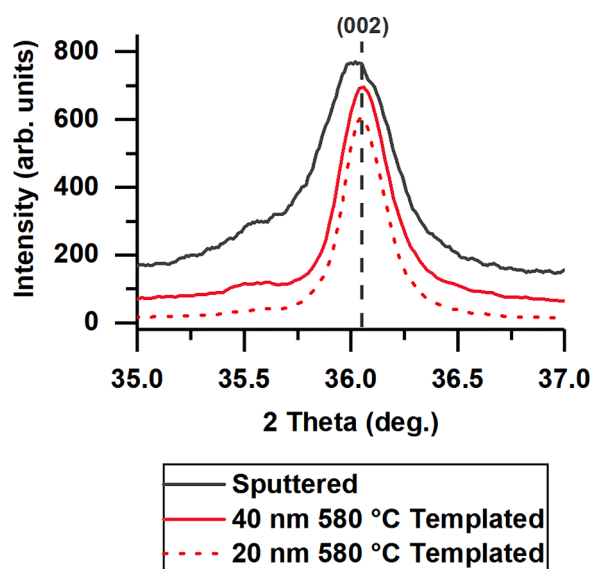


Fig. 8. Bragg-Brentano XRD comparison of the AlN (002) diffraction peaks of three films on 4H-SiC with 190 nm total thickness Bragg-Brentano XRD patterns of the AlN (002) diffraction peaks of three films on 4H-SiC with 190 nm total thickness. The first film is an entirely sputtered film with 0.38° FWHM; the second and third films are composed of 20 nm and 40 nm 580 °C pulsed CVD template layers followed by 170 nm and 150 nm of sputtered material, respectively. The second and third films have FWHM of 0.17° and 0.18°, respectively.

the 580 °C pulsed-CVD or 400 °C ALA templating layer, both with AlN (002) FWHM of 0.64°. The sputtered reference film has an AlN (002) FWHM of 0.79° and shows mixed AlN (002) and AlN (103) orientation which is not desirable for the intended applications. The increase in preferential AlN (002) orientation is likely the result of local domain epitaxy across the template-sputtered interface, as both the 580 °C pulsed CVD process and 400 °C ALA process have been shown to deposit films with AlN (002) orientation [22]. These results highlight that a templating layer deposited by pulsed CVD can be as effective as a templating layer deposited by the more complex ALA process in increasing the crystallinity of sputtered AlN.

3.3. Templated sputtered films on SiC

The crystallinity of sputtered material on 4H-SiC is also enhanced when grown on template layers deposited by the 580 °C pulsed CVD process. Shown in Fig. 8 is a Bragg-Brentano XRD comparison: the first film is comprised of 190 nm of AlN sputtered directly onto 4H-SiC, the second and third films are comprised of 20 and 40 nm of AlN deposited by the 580 °C pulsed CVD process which were brought to a total thickness of 190 nm with sputtered AlN. Relative to the reference sputtered film with 0.38° FWHM, the 20 and 40 nm templated films show drastically sharper peaks at 0.17° and 0.18° FWHM, respectively, indicating superior crystallinity of the templated films. This increase in crystallinity is particularly notable since the sample temperature during sputtering was below 100 °C.

The efficacy of the pulsed CVD templating layers on SiC are made clear by the TEM, SAED, and HR-TEM shown in Fig. 9. The 20 nm template layer deposited by the 580 °C CVD process is shown in Fig. 9a.

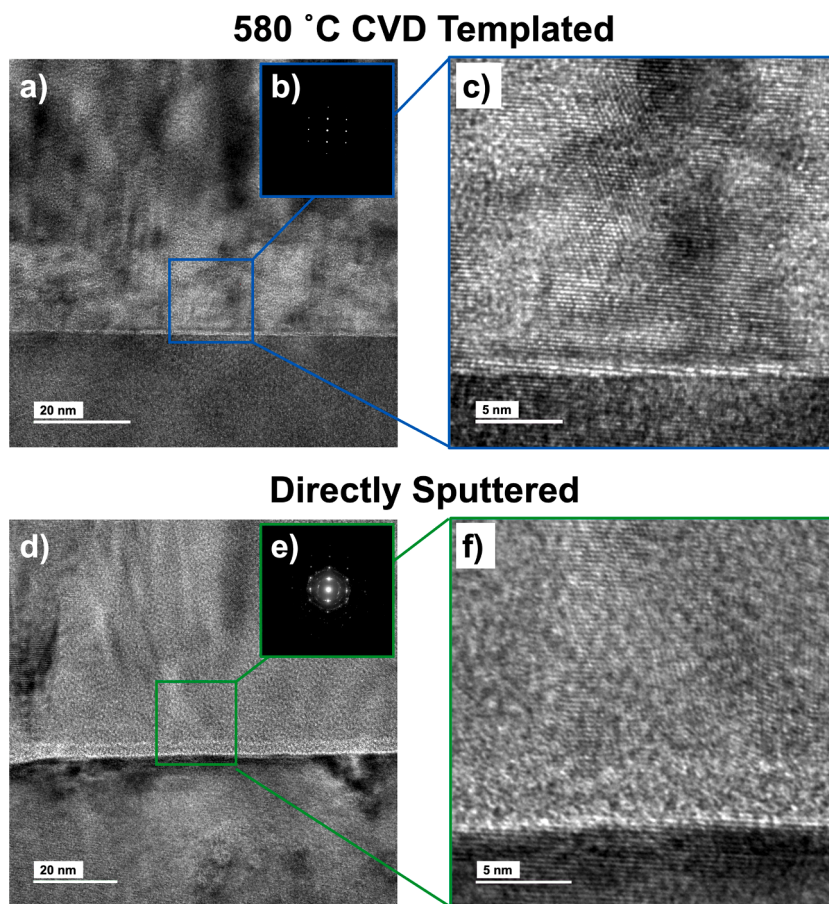


Fig. 9. Electron Microscopy Comparisons of a 580 °C Pulsed CVD Templated Film and a Directly Sputtered Film on SiC Substrates TEM, SAED, and HR-TEM, respectively, of the 20 nm 580 °C CVD templated film (a–c) and the directly sputtered film (d–f) on 4H-SiC substrates.

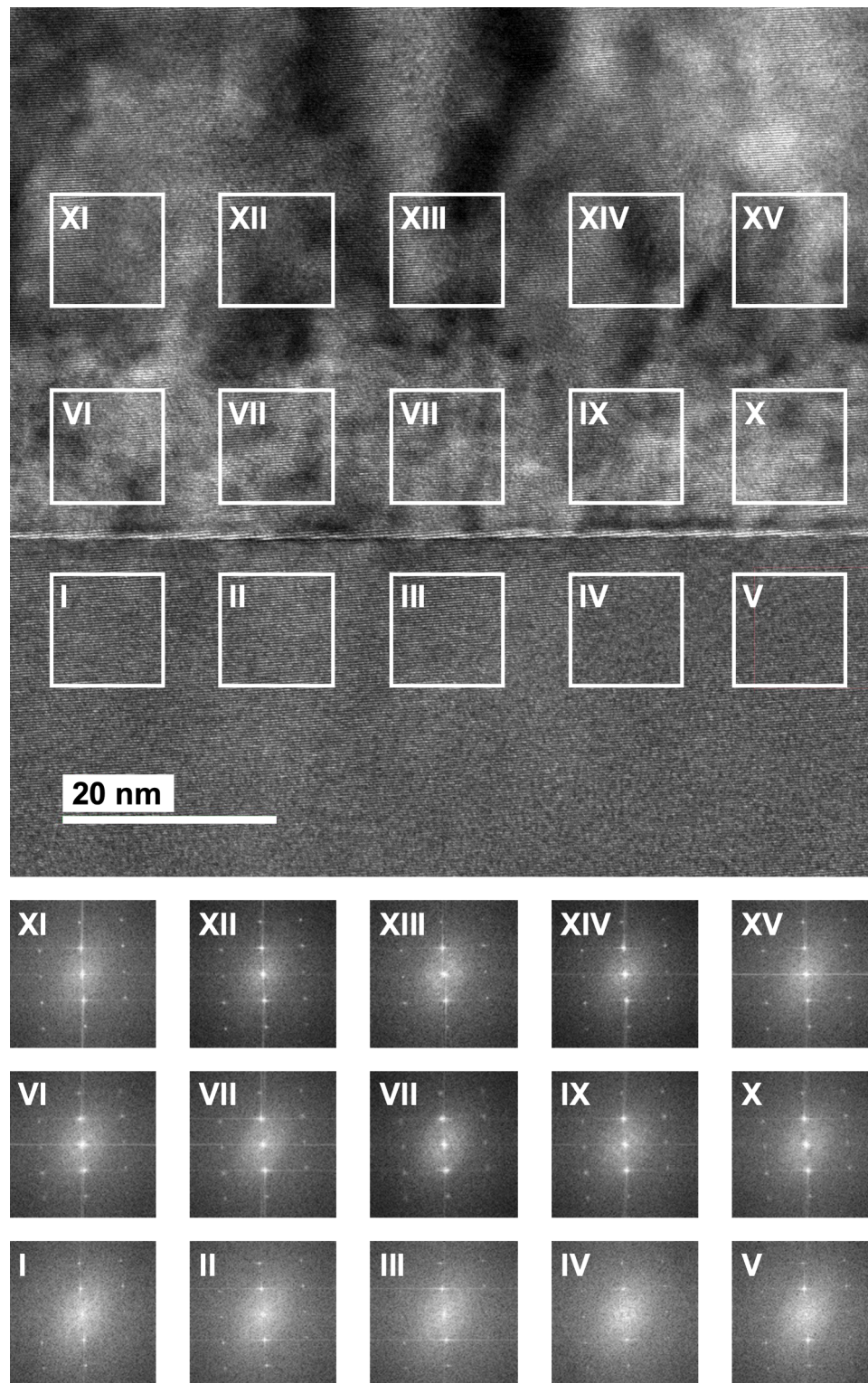


Fig. 10. Fast Fourier Transform Analysis of a CVD-Templated Film on SiC TEM image of the 20 nm 580 °C CVD templated - 170 nm sputtered AlN film on SiC with matching FFT patterns for the substrate (I-V), 580 °C CVD AlN layer (VI-X), and the sputtered AlN layer (XI-XV) at the bottom.

This CVD layer is grown epitaxially, as is demonstrated by the SAED pattern in Fig. 9b, which shows a single crystal-like pattern, and the HR-TEM shown in Fig. 9c, where the lattice fringes of the SiC and AlN appear regularly spaced and uninterrupted. In comparison, TEM of the directly sputtered film in Fig. 9d reveals an initial amorphous layer of ~3–4 nm thickness. Additionally, the SAED pattern shown in Fig. 9e reveals diffraction rings from a film of polycrystalline nature with grains

at various tilt angles relative to the SiC diffraction pattern. The HR-TEM (Fig. 9f) of this film more clearly shows this initial amorphous region, with crystallites developing quickly thereafter.

Further analysis of the epitaxial relationship of the CVD-templated sputtered film shown in Fig. 9a is shown in Fig. 10. Fast Fourier transform (FFT) analysis was performed from the HR-TEM image for five ~10 x 10 nm regions each of the substrate (I-V), the CVD layer (VI-X),

and the sputtered layer (XI-XV). Each of the FFT regions shows the expected pattern for the 4H-SiC and AlN wurtzite structures, with matching orientation along the c-axis. This indicates that the epitaxial relationship observed between the SiC substrate and the CVD AlN layer creates long-range order and effectively templates the sputtered AlN layer.

The epitaxial growth of the 580 °C CVD template layer may be the result of comparatively greater adatom mobility on the growth surface due to the considerably higher substrate temperature and slower growth rate. In comparison, the initial amorphous region of the directly sputtered film may be the result of the combined higher deposition rate and a comparatively colder initial growth surface as the SiC substrate was not actively heated during sputtering. These effects likely resulted in constrained surface adatom mobility. For films deposited on SiC, these XRD, TEM, and SAED results demonstrate that the enhancement mechanism of the sputtered material is not a function of the CVD template layer thickness, but rather is the result of sputtering AlN onto a highly crystalline and lattice-matched CVD template layer.

4. Conclusions

These results demonstrate that a 580 °C pulsed CVD process for aluminum nitride is a viable alternative to more complex techniques such as atomic layer annealing and techniques requiring substantially greater substrate temperatures, such as MBE and MOCVD. Using tris(dimethylamido) aluminum and anhydrous hydrazine, crystalline films with low oxygen and carbon content can be achieved at temperatures as low as 400 °C, though substantial improvement in crystallinity and density is observed at 580 °C. When performed on SiC substrates, the 580 °C process demonstrates an epitaxial relationship with the substrate and forms a single crystal; this greatly enhances the crystallinity of reactively sputtered AlN with no active substrate heating. This technique may find use for the growth of crystalline AlN buffer layers for GaN and InGaN on silicon and silicon carbide, enabling a decrease in substrate costs for RF power electronics and for thermally conductive buffer layers for microLED devices.

CRedit authorship contribution statement

Aaron J. McLeod: Conceptualization, Investigation, Data curation, Formal analysis, Writing – original draft, Writing – review & editing, Visualization. **Scott T. Ueda:** Conceptualization, Investigation, Data curation. **Ping C. Lee:** Investigation, Data curation. **Jeff Spiegelman:** Resources, Supervision. **Ravindra Kanjolia:** Resources, Supervision. **Mansour Moinpour:** Resources, Supervision. **Jacob Woodruff:** Resources, Supervision. **Andrew C. Kummel:** Conceptualization, Writing – review & editing, Supervision, Project administration, Funding acquisition.

Declaration of Competing Interest

The authors declare that they have no known competing financial interests or personal relationships that could have appeared to influence the work reported in this paper.

Andrew Kummel reports financial support was provided by Semiconductor Research Corp. Andrew Kummel reports equipment, drugs, or supplies was provided by EMD Electronics. Andrew Kummel reports equipment, drugs, or supplies was provided by Rasirc, Inc.

Data availability

Data will be made available on request.

Acknowledgments

This work was supported in part by the Applications and Systems-Driven Center for Energy Efficient Integrated Nano Technologies (ASCENT), one of six centers in the Joint University Microelectronics Program (JUMP), an SRC program sponsored by the Defense Advanced Research Program Agency (DARPA). This work was performed in part at the San Diego Nanotechnology Infrastructure (SDNI) at UC San Diego, a member of the National Nanotechnology Coordinate Infrastructure, which is supported by the National Science Foundation (ECCS-1542148). The authors would like to thank EMD Performance Materials and Rasirc Matheson for supplying precursors.

References

- [1] R.L. Xu, M. Munõz Rojo, S.M. Islam, A. Sood, B. Vareskic, A. Katre, N. Mingo, K. E. Goodson, H.G. Xing, D. Jena, E. Pop, Thermal conductivity of crystalline AlN and the influence of atomic-scale defects, *J. Appl. Phys.* 126 (2019), <https://doi.org/10.1063/1.5097172>.
- [2] J.C. Nipko, C.K. Loong, Phonon excitations and related thermal properties of aluminum nitride, *Phys. Rev. B* 57 (1998) 10550–10554, <https://doi.org/10.1103/PhysRevB.57.10550>.
- [3] A. Franco Júnior, D.J. Shanfield, Thermal conductivity of polycrystalline aluminum nitride (AlN) ceramics, *Cerâmica* 50 (2004), <https://doi.org/10.1590/s0366-69132004000300012>.
- [4] Y.J. Heo, H.T. Kim, K.J. Kim, S. Nahm, Y.J. Yoon, J. Kim, Enhanced heat transfer by room temperature deposition of AlN film on aluminum for a light emitting diode package, *Appl. Therm. Eng.* (2013) 799–804, <https://doi.org/10.1016/j.applthermaleng.2012.07.024>.
- [5] L. la Spina, E. Iborra, H. Schellevis, M. Clement, J. Olivares, L.K. Nanver, Aluminum nitride for heatspreading in RF IC's, *Solid State Electron.* 52 (2008) 1359–1363, <https://doi.org/10.1016/j.sse.2008.04.009>.
- [6] J.W. Lee, S.H. Jung, H.Y. Shin, I.H. Lee, C.W. Yang, S.H. Lee, J.B. Yoo, Effect of buffer layer on the growth of GaN on Si substrate, *J. Cryst. Growth* 237 (2002) 1094–1098, [https://doi.org/10.1016/S0022-0248\(01\)02097-8](https://doi.org/10.1016/S0022-0248(01)02097-8).
- [7] B.H. Kang, J.E. Lee, D.S. Kim, S. Bae, S. Jung, J. Park, J. Jhin, D. Byun, Effect of amorphous and crystalline AlN buffer layers deposited on patterned sapphire substrate on GaN film quality, *J. Nanosci. Nanotechnol.* 16 (2016), <https://doi.org/10.1166/jnn.2016.13552>.
- [8] M. Sumiya, K. Fukuda, S. Yasiro, T. Honda, Influence of thin MOCVD-grown GaN layer on underlying AlN template, *J. Cryst. Growth* 532 (2020), <https://doi.org/10.1016/j.jcrysgro.2019.125376>.
- [9] A.C. Jones, S.A. Rushworth, D.J. Houlton, J.S. Roberts, V. Roberts, C. R. Whitehouse, G.W. Critchlow, Deposition of aluminum nitride thin films by MOCVD from the trimethylaluminum-ammonia adduct, *Chem. Vap. Depos.* 2 (1996), <https://doi.org/10.1002/cvde.19960020102>.
- [10] S. Yoshida, S. Misawa, Y. Fujii, S. Takada, H. Hayakawa, S. Gonda, A. Itoh, Reactive molecular beam epitaxy of aluminium nitride, *J. Vac. Sci. Technol.* 16 (1979), <https://doi.org/10.1116/1.570166>.
- [11] C.R. Eddy, T.J. Anderson, A.D. Koehler, N. Nepal, D.J. Meyer, M.J. Tadjer, R. Baranyai, J.W. Pomeroy, M. Kuball, T.I. Feygelson, B.B. Pate, M.A. Mastro, J. K. Hite, M.G. Ancona, F.J. Kub, K.D. Hobart, GaN power transistors with integrated thermal management, *ECS Trans.* 58 (2013), <https://doi.org/10.1149/05804.0279ecst>.
- [12] L. Shen, S. Heikman, B. Moran, R. Coffie, N.Q. Zhang, D. Buttari, I.P. Smorchkova, S. Keller, S.P. DenBaars, U.K. Mishra, AlGaIn/AlN/GaN high-power microwave HEMT, *IEEE Electron Device Lett.* 22 (2001), <https://doi.org/10.1109/55.954910>.
- [13] M. Bosund, T. Sajaavaara, M. Laitinen, T. Huhtio, M. Putkonen, V.M. Airaksinen, H. Lipsanen, Properties of AlN grown by plasma enhanced atomic layer deposition, *Appl. Surf. Sci.* 257 (2011), <https://doi.org/10.1016/j.apsusc.2011.04.037>.
- [14] P. Motamedi, K. Cadien, XPS analysis of AlN thin films deposited by plasma enhanced atomic layer deposition, *Appl. Surf. Sci.* 315 (2014), <https://doi.org/10.1016/j.apsusc.2014.07.105>.
- [15] M. Legallais, H. Mehdi, S. David, F. Bassani, S. Labau, B. Pelissier, T. Baron, E. Martinez, G. Ghibaudo, B. Salem, Improvement of AlN film quality using plasma enhanced atomic layer deposition with substrate biasing, *ACS Appl. Mater. Interfaces* 12 (2020), <https://doi.org/10.1021/acsami.0c10515>.
- [16] H.Y. Shih, W.H. Lee, W.C. Kao, Y.C. Chuang, R.M. Lin, H.C. Lin, M. Shiojiri, M. J. Chen, Low-temperature atomic layer epitaxy of AlN ultrathin films by layer-by-layer, in-situ atomic layer annealing, *Sci. Rep.* 7 (2017), <https://doi.org/10.1038/srep39717>.
- [17] W.H. Lee, W.C. Kao, Y.T. Yin, S.H. Yi, K.W. Huang, H.C. Lin, M.J. Chen, Subnanometer heating depth of atomic layer annealing, *Appl. Surf. Sci.* 525 (2020), <https://doi.org/10.1016/j.apsusc.2020.146615>.
- [18] A.I. Abdulagatov, R.R. Amashaev, K.N. Ashurbekova, K.N. Ashurbekova, M. K. Rabadanov, I.M. Abdulagatov, Atomic layer deposition of aluminum nitride and oxynitride on silicon using tris(dimethylamido)aluminum, Ammonia, and Water, *Russ. J. Gen. Chem.* 88 (2018), <https://doi.org/10.1134/S1070363218080236>.
- [19] Y.C. Jung, S.M. Hwang, D.N. Le, A.L.N. Kondusamy, J. Mohan, S.W. Kim, J.H. Kim, A.T. Lucero, A. Ravichandran, H.S. Kim, S.J. Kim, R. Choi, J. Ahn, D. Alvarez, J. Spiegelman, J. Kim, Low temperature thermal atomic layer deposition of

- aluminum nitride using hydrazine as the nitrogen source, *Materials* 13 (2020), <https://doi.org/10.3390/ma13153387>. Basel.
- [20] D. Riihelä, M. Ritala, R. Matero, M. Leskelä, J. Jokinen, P. Haussalo, Low temperature deposition of AlN films by an alternate supply of trimethyl aluminum and ammonia, *Chem. Vap. Depos.* 2 (1996), <https://doi.org/10.1002/cvde.19960020612>.
- [21] S.C. Buttera, D.J. Mandia, S.T. Barry, Tris(dimethylamido)aluminum(III): an overlooked atomic layer deposition precursor, *J. Vac. Sci. Technol. A Vac. Surf. Films* 35 (2017), <https://doi.org/10.1116/1.4972469>.
- [22] S.T. Ueda, A. McLeod, D. Alvarez, D. Moser, R. Kanjolia, M. Moinpour, J. Woodruff, A.C. Kummel, Tris(dimethylamido)aluminum(III) and N₂H₄: ideal precursors for the low-temperature deposition of large grain, oriented c-axis AlN on Si via atomic layer annealing, *Appl. Surf. Sci.* 554 (2021), <https://doi.org/10.1016/j.apsusc.2021.149656>.
- [23] G. Liu, E. Deguns, L. Lecordier, G. Sundaram, J. Becker, Atomic layer deposition of AlN with tris(dimethylamido)aluminum and NH₃, *ECS Trans.* 41 (2011), <https://doi.org/10.1149/1.3633671>.
- [24] L. Rosenberger, R. Baird, E. McCullen, G. Auner, G. Shreve, XPS analysis of aluminum nitride films deposited by plasma source molecular beam epitaxy, *Surf. Interface Anal.* 40 (2008) 1254–1261, <https://doi.org/10.1002/sia.2874>.
- [25] J.X. Zhang, H. Cheng, Y.Z. Chen, A. Uddin, S. Yuan, S.J. Geng, S. Zhang, Growth of AlN films on Si (100) and Si (111) substrates by reactive magnetron sputtering, *Surf. Coat. Technol.* 198 (2005) 68–73, <https://doi.org/10.1016/j.surfcoat.2004.10.075>.
- [26] S.T. Ueda, A. McLeod, Y. Jo, Z. Zhang, J. Spiegelman, J. Spiegelman, D. Alvarez, D. Moser, R. Kanjolia, M. Moinpour, J. Woodruff, K. Cho, A.C. Kummel, Experimental and theoretical determination of the role of ions in atomic layer annealing, *J. Mater. Chem. C Mater.* (2022), <https://doi.org/10.1039/D1TC05194F>.